Thermoelectric properties of mesoscopic superconductors

N. R. Claughton and C. J. Lambert
School of Physics and Chemistry, Lancaster University, Lancaster, LA1 4YB, England
(Received 4 August 1995; revised manuscript received 6 November 1995)

We develop a general framework for describing thermoelectric effects in phase-coherent superconducting structures. Formulas for the electrical conductance, thermal conductance, thermopower, and Peltier coefficient are obtained and their various symmetries discussed. Numerical results for both dirty and clean Andreev interferometers are presented. We predict that giant oscillations of the thermal conductance can occur, even when oscillations in the electrical conductance are negligibly small. Results for clean, two-dimensional systems with a single superconducting inclusion are also presented, which show that normal-state oscillations arising from quasiparticle boundary scattering are suppressed by the onset of superconductivity. In contrast, for a clean system with no normal-state boundary scattering, switching on superconductivity induces oscillations in off-diagonal thermoelectric coefficients.

I. INTRODUCTION

The past few years have seen a rapid growth of interest in quantum transport through nanoscale superconductors and normal-superconducting contacts. In such devices, a variety of superconductivity-enhanced quasiparticle, interference effects (SEQUIN's) have either been observed[1–12] or are predicted.[13–31] These include results for zero-bias anomalies, quantization of the supercurrent in Josephson point contacts, anomalous proximity effects, and Andreev interferometers. In the latter, which are formed from a phase-coherent nanostructure in contact with two superconductors, with superconducting order parameter phases ϕ_1,ϕ_2, the electrical conductance is observed to be an oscillatory function of the externally controllable phase difference $\phi=\phi_1-\phi_2$.[1–4]

Attention to data has centered almost exclusively on charge transport measurements, which in the absence of strong correlations, can be understood using quasiparticle scattering theories. The aim of this paper is to develop a theory of thermoelectric effects in nanoscale superconductors. Thermoelectric properties of normal-state nanostructures have already been discussed in the literature[32–35] and when superconductivity is absent, the results of these theories are recovered from the framework developed below. In the presence of superconductivity, the theory is strongly modified by Andreev scattering, whereby a particlelike excitation can coherently evolve into a hole and during which energy, but not quasiparticle charge is conserved. As a consequence of this charge-energy separation, superconductors are excellent electrical conductors, but poor thermal conductors.[36]

The formalism developed below is very general and describes systems containing finite-size superconducting islands, as well as systems attached to superconducting reservoirs. After deriving general current-voltage relations, various limits are discussed. As an example, at low enough temperatures, for a hybrid structure in contact with two normal reservoirs at potentials v_1,v_2 and temperatures T_1,T_2, we demonstrate that to lowest order in v_i-v, T_1-T_2, these reduce to

$$\begin{pmatrix} I_1 \\ I_2 \\ Q \end{pmatrix} = \begin{pmatrix} g_{11} & g_{12} & g_{13} \\ g_{21} & g_{22} & g_{23} \\ g_{31} & g_{32} & g_{33} \end{pmatrix} \begin{pmatrix} (v_1-v) \\ (v_2-v) \\ (T_1-T_2) \end{pmatrix}. \tag{1}$$

This result differs from more familiar current-voltage relations,[37] derived for normal-state conductors, because the condensate potential v appears explicitly on the right-hand side, reflecting the fact that the superconductor can act as a source and sink of charge.[38] On the other hand, in the absence of inelastic scattering, the condensate cannot act as a source or sink of energy and therefore the temperature of the superconductor is absent from Eq. (1).

In steady state, if no net current flows into the superconductor, then the condensate potential v is determined by the condition $I_1=-I_2=I$ and Eq. (1) reduces to

$$\begin{pmatrix} I \\ Q \end{pmatrix} = \begin{pmatrix} G & L \\ M & K \end{pmatrix} \begin{pmatrix} (v_1-v_2) \\ (T_1-T_2) \end{pmatrix}. \tag{2}$$

In the following section, expressions for the thermoelectric coefficients G,L,M,K are derived and various symmetries highlighted. In Sec. III we present numerical results for a two-dimensional structure containing a single superconducting inclusion and in Sec. IV, we examine the thermoelectric properties of Andreev interferometers.

II. EXPRESSIONS FOR THERMOELECTRIC COEFFICIENTS

In this section, we generalize a microscopic scattering approach,[38] which describes electrical properties of nanoscale superconductors connected to external reservoirs by normal or superconducting contacts. In the absence of inelastic scattering, dc transport is determined by the quantum-mechanical scattering matrix $s(E,H)$, which yields scattering properties of excitations at energy E, of a phase-coherent structure described by a Hamiltonian H. If the structure is connected to external reservoirs by open scattering channels labeled by quantum numbers n, then s-matrix elements $s_{n,n'}(E,H)$ are defined such that $|s_{n,n'}(E,H)|^2$ is the outgo-

ing flux of quasiparticles along channel n, arising from a unit incident flux along channel n'.

In what follows, we consider channels belonging to current-carrying leads, with quasiparticles labeled by a discrete quantum number α ($\alpha=+1$ for particles, -1 for holes) and therefore write $n=(l,\alpha)$, where l labels all other quantum numbers associated with the leads. With this notation, the scattering matrix elements $s_{n,n'}(E,H)=s^{\alpha,\beta}_{l,l'}(E,H)$ satisfy $s^{\dagger}(E,H)=s^{-1}(E,H), s^{t}(E,H)=s(E,H^{*})$ and if E is measured relative to the condensate chemical potential $\mu=ev$, $s^{\alpha,\beta}_{l,l'}(E,H)=\alpha\beta[s^{-\alpha,-\beta}_{l,l'}(-E,H)]^{*}$. For a scatterer connected to external reservoirs by L crystalline, normal leads, labeled $i=1,2,\ldots,L$, and L_s superconducting leads labeled $i=L+1,\ldots,L+L_s$, it is convenient to write $l=(i,a)$, $l'=(j,b)$, where $a(b)$ is a channel belonging to lead $i(j)$ and focus attention on the quantity

$$P^{\alpha,\beta}_{i,j}(E,H)=\sum_{a,b}|s^{\alpha,\beta}_{(i,a),(j,b)}(E,H)|^2, \tag{3}$$

which is referred to as either a reflection probability ($i=j$) or a transmission probability ($i\neq j$) for quasiparticles of type β from lead j to quasiparticles of type α in lead i. For $\alpha\neq\beta$, $P^{\alpha,\beta}_{i,j}(E,H)$ is referred to as an Andreev scattering probability, while for $\alpha=\beta$, it is a normal scattering probability. Since unitarity yields

$$\sum_{\beta bj}|s^{\alpha,\beta}_{(i,a),(j,b)}(E,H)|^2=\sum_{\alpha aj}|s^{\alpha,\beta}_{(i,a),(j,b)}(E,H)|^2=1, \tag{4}$$

where i and j sum only over leads containing open channels of energy E, this satisfies

$$\sum_{\substack{\beta\\ j=1}}^{L+L_s}P^{\alpha,\beta}_{ij}(E,H)=N^{\alpha}_{i}(E)\quad\text{and}\quad\sum_{\substack{\alpha\\ i=1}}^{L+L_s}P^{\alpha,\beta}_{ij}(E,H)=N^{\beta}_{j}(E), \tag{5}$$

where $N^{\alpha}_{i}(E)$ is the number of open channels for α-type quasiparticles of energy E in lead i, satisfying $N^{+}_{i}(E)=N^{-}_{i}(-E)$. For convenience, if a lead i contains no open channels of energy E, we define $P^{\alpha,\beta}_{ij}(E,H)=P^{\alpha,\beta}_{ji}(E,H)=0$ and in Eqs. (4) and (5) sum over all i and j.

To compute the current I_i and heat flux Q_i into a normal lead i, it is convenient to introduce the notation $I^{0}_{i}=I_i/e$ and $I^{1}_{i}=-Q_i$. Then for a system connected to external reservoirs at potentials v_i and temperatures T_i, one finds[38,39]

$$I^{p}_{i}=\sum_{j=1}^{L+L_s}\bar{A}^{p}_{ij}\quad(i=1,2,\ldots,L), \tag{6}$$

where

$$\bar{A}^{p}_{i,j\neq i}=(-2/h)\sum_{\alpha\beta}(\alpha)^{(1-p)}\int_0^{\infty}dE\;E^{p}P^{\alpha\beta}_{ij}(E,H)f^{\beta}_{j}(E), \tag{7}$$

$$\bar{A}^{p}_{ii}=(2/h)\sum_{\alpha}(\alpha)^{(1-p)}\int_0^{\infty}dE\;E^{p}\left(N^{\alpha}_{i}(E)f^{\alpha}_{i}(E)-\sum_{\beta}P^{\alpha\beta}_{ii}(E,H)f^{\beta}_{i}(E)\right) \tag{8}$$

and $f^{\alpha}_{j}(E)=(\exp\{[E-\alpha(ev_j-\mu)]/k_bT_j\}+1)^{-1}$ is the distribution of incoming α-type quasiparticles from lead j. To avoid time-dependent order parameter phases varying at the Josephson frequency, which would render a time-independent scattering approach invalid, we insist that all superconductors share a common condensate chemical potential μ and therefore for $j>L$, choose $ev_j=\mu$.

Once the currents in the normal leads are known, the total currents $I_0=\Sigma_{i=L+1}^{L+L_s}I_i$, $Q_0=\Sigma_{i=L+1}^{L+L_s}Q_i$ flowing in the superconductor(s) are given by $I_0+\Sigma_{i=1}^{L}I_i=0$, $Q_0+\Sigma_{i=1}^{L}Q_i=0$. Equation (6) yields the current-voltage characteristics of a given structure at finite voltages, provided all scattering coefficients are computed in the presence of a self-consistently determined order parameter. Such calculations have been carried out recently for one-dimensional structures[30,31] and demonstrate that provided the currents are low enough, the matrix $P^{\alpha\beta}_{ij}(E,H)$ can remain unchanged, even by the application of finite voltages of order Δ_0. In this case, expanding Eqs. (7) and (8) to lowest order in $\mu_j-\mu$ and T_j-T yields

$$I^{p}_{i}=\sum_{j=1}^{L}B^{p}_{ij}(\mu_j-\mu)+\sum_{j=1}^{L+L_s}C^{p}_{ij}(T_j-T)\quad(i=1,2,\ldots,L), \tag{9}$$

where

$$B^{p}_{i,j\neq i}=(-2/h)\sum_{\alpha\beta}(\alpha)^{(1-p)}\beta\int_0^{\infty}dE\;E^{p}\left(\frac{-\partial f}{\partial E}\right)P^{\alpha\beta}_{ij}(E,H), \tag{10}$$

$$B^{p}_{ii}=(2/h)\sum_{\alpha\beta}(\alpha)^{(1-p)}\beta\int_0^{\infty}dE\;E^{p}\left(\frac{-\partial f}{\partial E}\right)[N^{\alpha}_{i}(E)\delta_{\alpha\beta}-P^{\alpha\beta}_{ii}(E,H)], \tag{11}$$

$$C^{p}_{i,j\neq i}=(-2/h)\sum_{\alpha\beta}(\alpha)^{(1-p)}\int_0^{\infty}dE\,\frac{E^{p+1}}{T}\left(\frac{-\partial f}{\partial E}\right)P^{\alpha\beta}_{ij}(E,H), \tag{12}$$

$$C^{p}_{ii}=(2/h)\sum_{\alpha\beta}(\alpha)^{(1-p)}\int_0^{\infty}dE\,\frac{E^{p+1}}{T}\left(\frac{-\partial f}{\partial E}\right)[N^{\alpha}_{i}(E)\delta_{\alpha\beta}-P^{\alpha\beta}_{ii}(E,H)], \tag{13}$$

and $f(E)=\{\exp[E/k_bT]+1\}^{-1}$.

The above current-voltage relation is a key result of this paper. If the matrix elements $P^{\alpha\beta}_{ij}(E,H)$ vary significantly over the energy range k_BT, then the integrals must be evaluated without further approximation. On the other hand if k_BT is small enough, one can proceed as in the following section, by Taylor expanding in energy and retaining only the lowest nonzero terms.

It is interesting that the temperature T has not yet been specified, whereas the parameter μ is identified with the

unique condensate chemical potential. An important feature of Eq. (9) is obtained by noting that in view of the unitarity condition (5),

$$\sum_{j=1}^{L+L_s} C_{ij}^p = (2/h)\sum_{\alpha} (\alpha)^{(1-p)} \int_0^{\infty} dE \frac{E^{p+1}}{T}\left(\frac{-\partial f}{\partial E}\right) \times\left(N_i^{\alpha} - \sum_{\substack{\beta \\ j=1}} P_{ii}^{\alpha\beta}(E,H)\right). \tag{14}$$

Hence the explicit dependence on the temperature T drops out from Eq. (9). In contrast, in the presence of Andreev scattering, the coefficients B_{ij}^p satisfy no such sum rule and the explicit dependence on μ remains. The only requirement on T is that it is in the vicinity of the reservoir temperatures T_i, so that higher-order terms in the Sommerfeld expansions of B_{ij}^p, C_{ij}^p can be neglected. In practice it may be convenient to equate T to one of the reservoir temperatures.

III. EXPRESSIONS FOR THERMOELECTRIC COEFFICIENTS IN THE LOW-TEMPERATURE LIMIT

We now consider the low-temperature limit, in which the contribution from any open channels in the superconductors is negligible and the lowest terms in a Taylor expansion is a good approximation to the right-hand sides of Eqs. (15)–(18). For convenience, we restrict the analysis to two normal probes of identical cross section, for which a more intuitive notation can be employed. Open channels in the superconductor(s) are negligible when superconducting leads are absent (i.e., $L_s=0$) or when k_BT is much lower than the superconducting energy gap of any superconducting leads. In this case $C_{ij}^p=0$ for $j>L$ and for $L=2$, Eq. (14) yields $C_{i2}^p=-C_{i1}^p$. Hence Eq. (9) reduces to

$$I_i^p = \sum_{j=1}^{2} B_{ij}^p(\mu_j-\mu) + C_{i1}^p(T_1-T_2) \quad (i=1,2,\ldots,L), \tag{15}$$

which is of the form of Eq. (1).

Introducing the parameters

$$a \equiv \frac{\pi^2}{3}\frac{1}{e}k_B^2 T, \tag{16}$$

$$b \equiv \frac{\pi^2}{3}\frac{1}{e}k_B^2 T^2 = aT, \tag{17}$$

$$c \equiv \frac{\pi^2}{3}\frac{1}{e^2}k_B^2 T = a/e, \tag{18}$$

yields for the conductance matrix of Eq. (1),

$$g = \begin{pmatrix} g_{11} & g_{12} & g_{13} \\ g_{21} & g_{22} & g_{23} \\ g_{31} & g_{32} & g_{33} \end{pmatrix} = \frac{2e^2}{h}\begin{pmatrix} \begin{bmatrix} N+R_a-R_0 & T_a'-T_0' \\ T_a-T_0 & N+R_a'-R_0' \end{bmatrix} & a\begin{bmatrix} \tilde{R}_a-\tilde{R}_0 \\ \tilde{T}_a-\tilde{T}_0 \end{bmatrix} \\ -b[(\tilde{T}_0+\tilde{T}_a)-(\tilde{T}_a'+\tilde{T}_0')] & -c[T_0+T_a] \end{pmatrix}. \tag{19}$$

In this expression, a tilde represents the derivative with respect to energy, $R_0=P_{11}^{++}(0,H)$, $T_0=P_{21}^{++}(0,H)$ $[R_a=P_{11}^{-+}(0,H), T_a=P_{21}^{-+}(0,H)]$ are probabilities for normal (Andreev) reflection and transmission for quasiparticles from reservoir 1, while R_0', T_0' (R_a', T_a') are corresponding probabilities for quasiparticles from reservoir 2. The number of open channels per lead is $N=N_1^+(0)=N_2^+(0)$ and from Eqs. (5), $R_0+T_0+R_a+T_a=R_0'+T_0'+R_a'+T_a'=N$ and $T_0+T_a=T_0'+T_a'$.

In principle, through the response to independent variations in the quantities v_i-v and T_i-T_2, all nine matrix elements are measurable. For the case where the steady-state condition $I_1=-I_2=I$ is satisfied, Eq. (2) is obtained, with

$$G = (T_0+T_a) + 2\left\{\frac{R_aR_a'-T_aT_a'}{R_a+R_a'+T_a+T_a'}\right\}, \tag{20}$$

$$L/a = (\tilde{T}_0'-\tilde{T}_a') - 2\left\{\frac{(\tilde{R}_a+\tilde{T}_a)(R_a+T_a')}{R_a+R_a'+T_a+T_a'}\right\}, \tag{21}$$

$$-M/b = (\tilde{T}_0+\tilde{T}_a) + 2\left\{\frac{(R_a+T_a)(\tilde{R}_a+\tilde{T}_a')}{R_a+R_a'+T_a+T_a'}\right\}, \tag{22}$$

$$-K/c = (T_0+T_a) + 2\frac{ab}{c}\left\{\frac{(\tilde{R}_a+\tilde{T}_a)(\tilde{R}_a+\tilde{T}_a')}{R_a+R_a'+T_a+T_a'}\right\}. \tag{23}$$

In these expressions, every numerator is second order in Andreev coefficients, whereas the common denominator is first order. This ensures that the ratios are well behaved in the limit that the Andreev coefficients approach zero. These equations can of course be rewritten in many forms. For example, the first two expressions can be written

$$G = (N+R_a-R_0) - 2\left\{\frac{(R_a+T_a)(R_a+T_a')}{R_a+R_a'+T_a+T_a'}\right\}, \tag{24}$$

$$L/a = (\tilde{R}_a-\tilde{R}_0) - 2\left\{\frac{(\tilde{R}_a+\tilde{T}_a)(R_a+T_a')}{R_a+R_a'+T_a+T_a'}\right\}. \tag{25}$$

To highlight certain features of these expressions, it is instructive to write down the matrix elements in various limits. For example in the case of perfect left-right symmetry, where each primed coefficient is equal to the corresponding unprimed quantity, one obtains

$$G = T_0+R_a, \tag{26}$$

$$L/a = \tilde{T}_0+\tilde{R}_a, \tag{27}$$

$$M/b=\tilde{T}_0+\tilde{T}_a, \tag{28}$$

$$K/c=T_0+T_a. \tag{29}$$

As a second example, we note that in the absence of superconductivity, all Andreev terms vanish to yield

$$G=T_0, \tag{30}$$

$$L/a=\tilde{T}_0, \tag{31}$$

$$-M/b=\tilde{T}_0, \tag{32}$$

$$-K/c=T_0. \tag{33}$$

As a third example, we consider the case of a real order parameter, in the absence of a magnetic field. In this limit, time-reversal symmetry yields $\tilde{R}_a(0)=0$, $\tilde{R}'_a(0)=0$, $\tilde{T}_a(0)=-\tilde{T}'_a(0)$, and $\tilde{T}_0(0)=\tilde{T}'_0(0)$. Moreover, the P matrix is symmetric and therefore $T_a(0)=T'_a(0)$. Hence in this case,

$$G=(N+R_a-R_0)-2\left\{\frac{(R_a+T_a)(R_a+T'_a)}{R_a+R'_a+T_a+T'_a}\right\}, \tag{34}$$

$$L/a=-M/b=(\tilde{T}_0+\tilde{T}_a)-2\left\{\frac{\tilde{T}_a(R_a+T_a)}{R_a+R'_a+T_a+T'_a}\right\}, \tag{35}$$

$$-K/c=(T_0+T_a)-2\frac{ab}{c}\left\{\frac{\tilde{T}_a^2}{R_a+R'_a+T_a+T'_a}\right\}. \tag{36}$$

Equation (35) demonstrates that in the presence of time-reversal symmetry, the thermoelectric coefficients L and M are related by an Onsager relation

$$M=-TL. \tag{37}$$

Finally we note that in the most extreme case of a spatially symmetric structure possessing time-reversal symmetry, $\tilde{T}_a(0)=-\tilde{T}'_a(0)$ and $\tilde{T}_a(0)=+\tilde{T}'_a(0)$. Hence $\tilde{T}_a(0)=\tilde{T}'_a(0)=0$ and one finds $L/a=-M/b=\tilde{T}_0$, $-K/c=T_0+T_a$, $G=T_0+R_a$. An alternative way of expressing the above results is obtained by writing Eq. (2) in the form

$$\begin{pmatrix}(v_1-v_2)\\ Q\end{pmatrix}=\begin{pmatrix}R & S\\ \Pi & -\kappa\end{pmatrix}\begin{pmatrix}I\\ (T_1-T_2)\end{pmatrix}$$
$$=\begin{pmatrix}R & -RL\\ -RM & -K+MRL\end{pmatrix}\begin{pmatrix}I\\ (T_1-T_2)\end{pmatrix}, \tag{38}$$

where $R=1/G$ is the electrical resistance, $S\equiv(\Delta V/\Delta T)_{I=0}$ is the thermopower, $\Pi\equiv(Q/I)_{\Delta T=0}$ is the Peltier coefficient, and $\kappa\equiv-(Q/\Delta T)_{I=0}$ is the thermal conductance. In the presence of time-reversal symmetry, these reduce to $S=M/TG$, $\Pi=-TS$ and the thermal conductance κ and $\kappa=K(GTS^2/K+1)$. In the absence of superconductivity it can be seen from Eqs. (30)–(33) that

$$K=-cG=-L_0TG, \tag{39}$$

where $L_0=(k_B/e)^2\pi^2/3$ is the Lorentz number. If $S^2\ll L_0$ then $\kappa\approx K$ and one obtains the Weidemann-Franz law

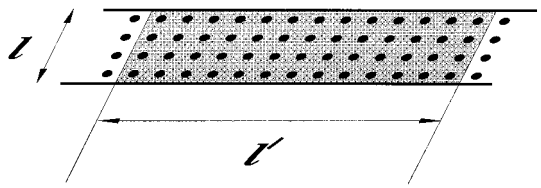

FIG. 1. A two-dimensional tight-binding system of width l sites and length l' sites (shown shaded) connected to normal, crystalline external leads of width l.

$$\kappa\approx L_0TG. \tag{40}$$

Clearly this breaks down in the presence of Andreev scattering.

IV. RESULTS FOR A SINGLE SUPERCONDUCTING INCLUSION

In this section, as a first application of the above theory, we present results for the thermoelectric coefficients G, L, M, and K, of a two-dimensional structure with a single superconducting inclusion. The aim is to examine the role of boundary scattering at N-S interfaces and therefore in this section, only clean structures will be considered. All results are obtained from numerical simulations of a two-dimensional tight-binding system, described by a Bogoliubov–de Gennes operator of the form

$$H=\begin{pmatrix}H_0 & \Delta\\ \Delta^* & -H_0^*\end{pmatrix}. \tag{41}$$

In this equation, H_0 is a nearest-neighbor Anderson model on a square lattice, with off-diagonal hopping elements of value $-\gamma$ and Δ is a diagonal order-parameter matrix. The scattering region is chosen to be l sites wide and l' sites long and is connected to external leads of width l as shown in Fig. 1. Within the scattering region, diagonal elements of H_0 are set to some value ϵ_1, while those of Δ are set equal to Δ_0. Within the leads, the diagonal elements of H_0 are equal to a constant ϵ_0, while those of Δ are set to zero. In what follows, for a given realization of the Hamiltonian H, the scattering matrix is obtained numerically, using a transfer matrix technique outlined in Appendix 2 of Ref. 39. All energy derivatives are calculated by obtaining the P matrix at $E=0$ and then again at $E=\Delta E$ where $\Delta E=10^{-6}$.

For the normalized thermoelectric coefficients defined by Eqs. (20)–(23) the temperature appears explicitly only in K/c, whose second term has a prefactor $ab/c=\pi^2/3(k_BT)^2$. The temperature T must be chosen to be sufficiently small that the Sommerfeld expansion leading to Eq. (1) remains valid and this holds if the energy scale over which the scattering matrix elements change is much larger than k_BT. In what follows we choose $k_BT=\delta E/8$, where δE is the level spacing $\delta E=8\gamma/(ll')$, which yields $ab/(c\gamma^2)\approx 3(ll')^{-2}$.

Figure 2 shows results for the thermal coefficients G, L/a, M/b, and K/c, computed for five values of the superconducting order parameter, namely $\Delta_0=0$, 0.01, 0.1, 0.3, and 0.5. For these calculations, the system is of width $l=10$, the choice $\gamma=1$ was made and ϵ_0 lies in the range

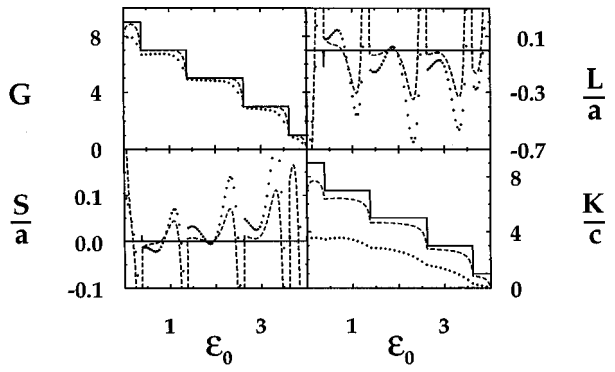

FIG. 2. The electrical conductance G (top left) and normalized thermal conductance K/c (bottom right) as a function of ϵ_0 for a clean system of width $l=10$ and length $l'=5$. The top right graph shows the normalized thermoelectric cross coefficients $L/a=M/b$ and the bottom left graph depicts the normalized thermopower S/a. Each separate curve refers to one of the following values of the superconducting order parameter: $\Delta_0=0$ (solid), 0.1 (dashed), and 0.3 (dotted).

$0.0\leqslant\epsilon_0/\gamma\leqslant 4.0$. In Fig. 2, the length of the superconductor is $l'=5$ and $\epsilon_1=\epsilon_0$. In the normal limit, where $\Delta_0=0$, the conductances $G=K/c$ exhibit a series of steps associated with the closing of scattering channels. From Eqs. (31) and (32), $L/a=M/b$ is the energy derivative of G and since, when $\Delta_0=0$, a shift in ϵ_0 is equivalent to a change in energy, each step in G is accompanied by a δ function in L/a and M/b. These δ functions cannot be discerned in the plots of Fig. 2. For finite Δ_0, the δ functions are smeared and L/a exhibits oscillations arising from the interference of quasiparticles from the two ends of the sample. With increasing Δ_0, the oscillations die away as the transmission coefficients and their derivatives become suppressed. Increasing Δ_0 also causes the conductance steps in G to become rounded and suppressed, in the manner of Fig. 9 of Ref. 22. A similar effect is observed in the coefficient K/c, but the suppression is more pronounced, due to the absence of Andreev scattering terms in Eq. (33). Figures 3 and 4 show a corresponding set of results for systems of length $l'=10$ and $l'=20$, respectively. These illustrate that increasing the length l' further suppresses K, but has little effect on G. They also illustrate that the frequency of oscillations in L/a and S/a

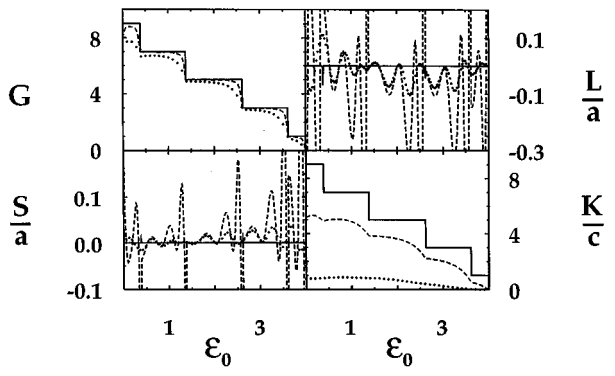

FIG. 3. As for Fig. 2, except the system is of length $l'=10$.

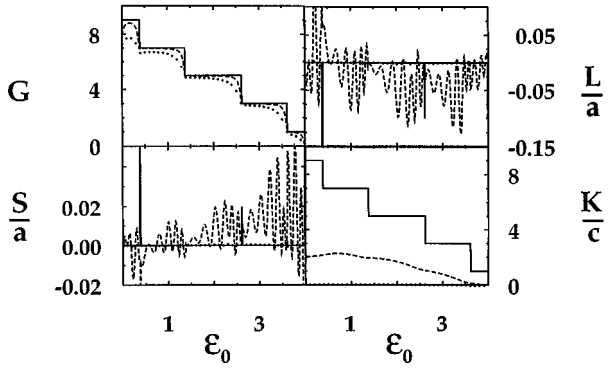

FIG. 4. As for Fig. 2, except the system is of length $l'=20$.

increases with increasing length, as expected for a quasiparticle interference effect of this kind.

The results of Figs. 2–4 show the effect of a global shift in the parameter ϵ_0, in the presence of a finite Δ_0. It is interesting to compare this with the behavior arising from a normal system in the absence of disorder, but with a Fermi-surface mismatch between the sample and the external leads. To simulate such a structure, Figs. 5–7 show results in the presence of a shift $\eta=\epsilon_1-\epsilon_0$ in the diagonal elements ϵ_1 of the superconducting region. For a system of length $l'=5$, Fig. 5 shows results for the variation of thermoelectric coefficients with the global constant ϵ_0, for eight different values of the mismatch parameter η. Figures 6 and 7 show corresponding results for systems of length $l'=10$ and $l'=20$, respectively. In each figure, $\gamma=1$, $l=10$, and ϵ_0 lies in the range $0.0\leqslant\epsilon_0/\gamma\leqslant 4.0$.

These figures illustrate that for a normal system, steps in G and K/c are suppressed by the introduction of a potential mismatch. They also illustrate that oscillations again arise from quasiparticle reflections at the boundaries and that the frequency of these oscillations increases as the system length increases. A crucial difference between the normal-state results of Figs. 5–7 and the superconducting results of Figs.

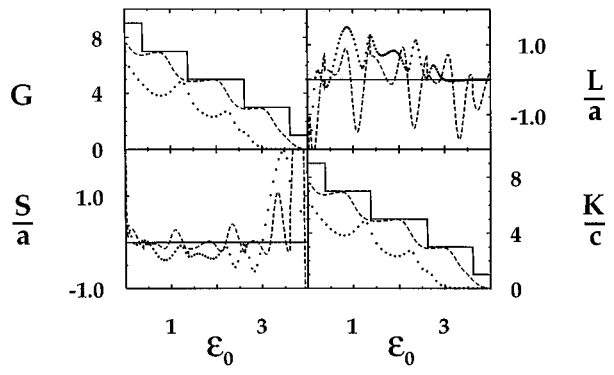

FIG. 5. The electrical conductance G (top left) and normalized thermal conductance K/c (bottom right) as a function of ϵ_0 for a clean system of width $l=10$ and length $l'=5$. The top right graph shows the normalized thermoelectric cross coefficients $L/a=M/b$ and the bottom left graph depicts the normalized thermopower S/a. Each separate curve refers to one of the following values of the parameter $\eta=\epsilon_1-\epsilon_0$: $\eta=0$ (solid), 0.3 (dashed), and 1.0 (dotted).

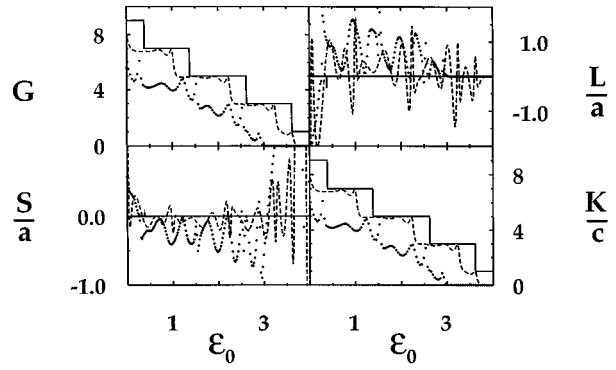

FIG. 6. As for Fig. 5, except the system is of length $l'=10$.

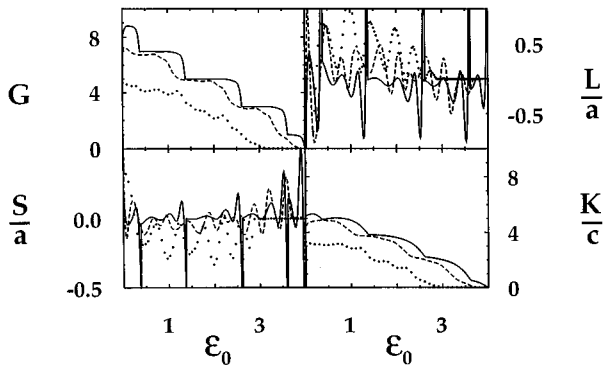

FIG. 8. The results shown here are an exact replica of those of Fig. 6 except that an order parameter of magnitude $\Delta_0=0.1$ has been switched on.

2–4, is that oscillations in G and K only occur in the former. Figure 8 shows the effect of the imposing a superconducting order parameter of magnitude $\Delta=0.1$ on the system of Fig. 6 and illustrates that switching on superconductivity suppresses oscillations associated with a Fermi-surface mismatch.

V. THERMOELECTRIC PROPERTIES OF ANDREEV INTERFEROMETERS

The numerical results of Sec. IV are merely a first, explicit realization of the formulas of Sec. III. In this section we examine thermoelectric properties of Andreev interferometers, formed from two superconductors with order-parameter phases ϕ_1,ϕ_2 in contact with a phase-coherent nanostructure. It is known[1–4,13–21] that the electrical conductance of such structures is a periodic function of the phase difference $\phi=\phi_1-\phi_2$, but no results for phase-periodic thermoelectric properties are currently available. Consider first the structure of Fig. 9, which comprises two superconducting islands, each of length l' sites and width l_s sites, with a uniform order parameter of magnitude $\Delta_0=0.1$. The transport current flows from left to right and apart from the order-parameter phase difference, the islands are identical. The islands are separated from each other by a normal region of width l_s sites, yielding a total system width of $l=3l_s$. Immediately adjacent the superconductor is a tunnel barrier of width l sites and thickness l_b sites. Within the barrier, the diagonal matrix elements ϵ_i are set to $\epsilon_0+\epsilon_b$, where ϵ_0 is the site energy in the leads and ϵ_b is a measure of the strength of the barrier. In every other region, the diagonal elements $\epsilon_i=\epsilon_0$.

For a barrier of thickness $l_b=1$, Fig. 10 shows numerical results for a system of width $l=15$ and three lengths $l'=5$ (solid line), $l'=15$ (open circles), and $l'=25$ (squares). Figures 10(a)–10(d) show results for barrier strengths of $\epsilon_b=0,1,2,3$, respectively. Since there is no disorder in these structures, in the absence of a barrier, the dominant scattering mechanism is either Andreev reflection or normal transmission. Both processes facilitate charge transport and therefore the electrical conductance exhibits only a small nonclassical amplitude of oscillation, which would be absent from quasiclassical theories of interferometers.[19,20] This small oscillation of amplitude $\ll 1$, is shown in the results for G as a function of ϕ, in Fig. 10(a). In contrast Andreev reflection impedes the flow of energy and as shown in Fig. 10(a), the thermal conductance K/c exhibits giant oscillations. By varying the width of the system, we find that the amplitude of these oscillations in K/c is proportional to the system width. Figures 10(b) and 10(c) show further that both L and S are periodic functions of ϕ, with period 2π and that the sign of these quantities is phase dependent. In the presence of a barrier, Figs. 10(b)–10(d) show that both K/c and G can exhibit large oscillations, which by increasing the system width, can again be shown to be proportional to l.

Figure 11 shows the same structure as Fig. 9, but with the tunnel barrier replaced by a diffusive normal region of length

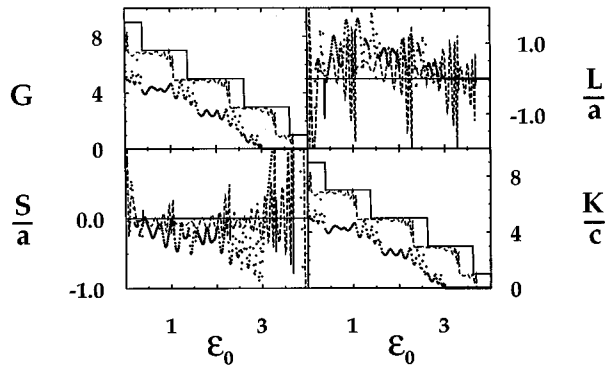

FIG. 7. As for Fig. 5, except the system is of length $l'=20$.

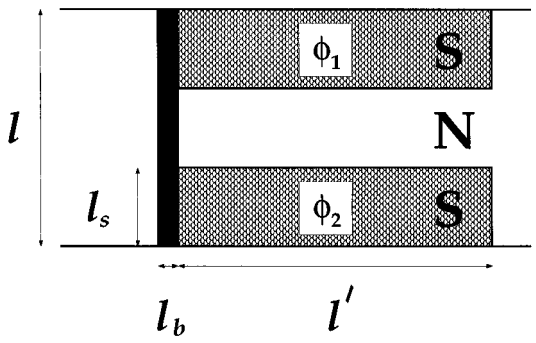

FIG. 9. A clean Andreev interferometer, with a tunnel barrier.

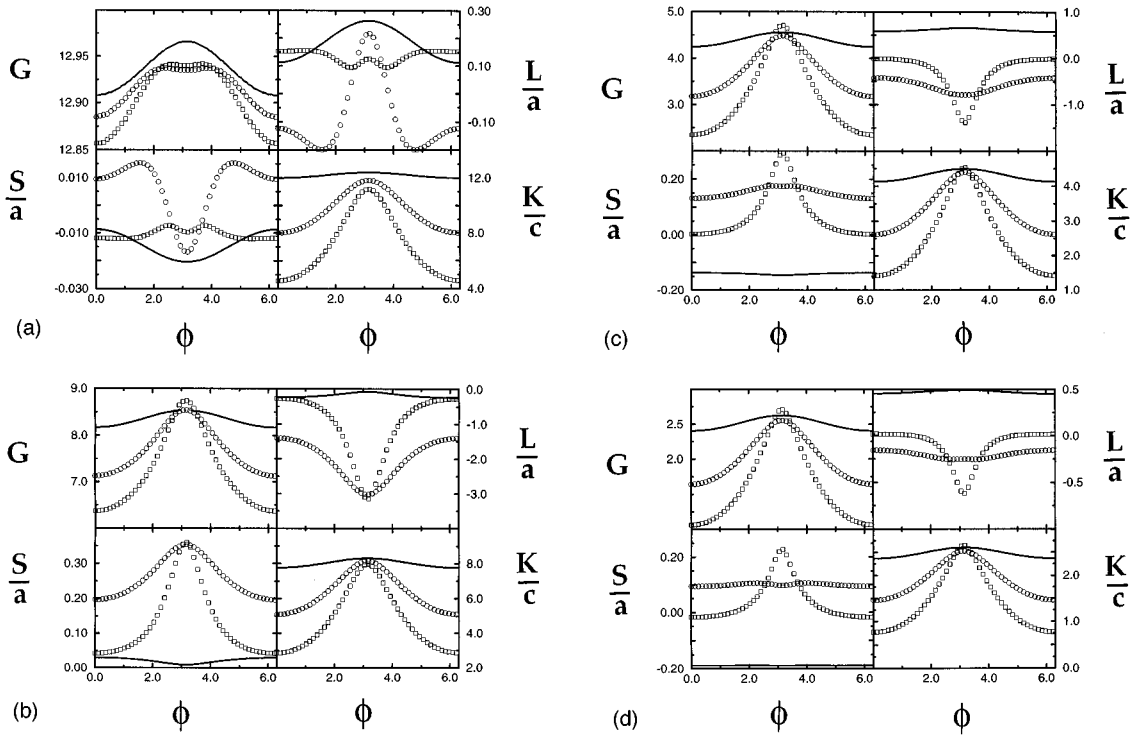

FIG. 10. (a)–(d) show results for barrier strengths of $\epsilon_b = 0$, 1, 2, 3, respectively. In each case, results are shown for samples of lengths $l' = 5$ (solid line), $l' = 15$ (open circles), and $l' = 25$ (squares).

l_d. Within the diffusive region, the elements ϵ_i are chosen to be uniformly distributed random numbers in the range $\epsilon_0 - W \leq \epsilon_i \leq \epsilon_0 + W$, where W is a measure of the strength of disorder. For a system of dimensions $l = l' = 15$ and $l_s = l_d = 5$, Fig. 12 shows results for $W = 1$, 2, and 3. For each value of W, thermoelectric coefficients were calculated as a function of ϕ, for 50 different realizations of the disorder. Figure 12 shows the ensemble averages of these results.

It should be noted that while K and G are necessarily even functions of ϕ, there is no such constraint on L and S and indeed results for individual realizations of the disorder are nonsymmetric about $\phi = 0$. One exception to this is for a system with a mirror symmetry about a horizontal line dividing the two superconductors, since in this case reversing the phase is equivalent to reflecting the sample and therefore cannot change any physical parameter. For the structure of Fig. 11, this symmetry is broken for a given realization of the disorder, but not on the average. Consequently the average values of L and S are even functions of ϕ. To illustrate the breaking of this symmetry, Fig. 13 shows a clean system with no barrier of dimensions $l = l' = 3l_s = 9$, but with the magnitude of the order parameter of the upper (lower) island set to 0.1 (0.7). Both L and S are manifestly nonsymmetric about $\phi = 0$, whereas G and κ remain even functions of ϕ.

VI. CONCLUSION

We have developed a general framework for describing thermoelectric effects in phase-coherent superconducting structures. At low temperatures, the general current-voltage relation of Eq. (16) reduces to the linear-response formula of

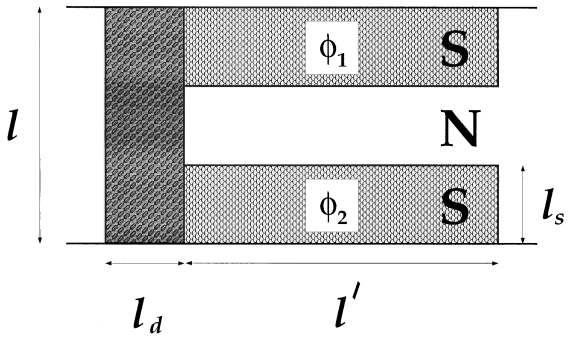

FIG. 11. An Andreev interferometer, with a diffusive normal region located to the left of the superconductors. All other regions are free from disorder.

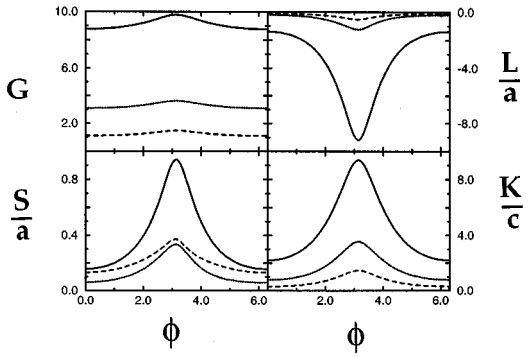

FIG. 12. Results obtained for the structure of Fig. 11, for $W = 1$ (solid line), $W = 2$ (dotted line), and $W = 3$ (dashed line).

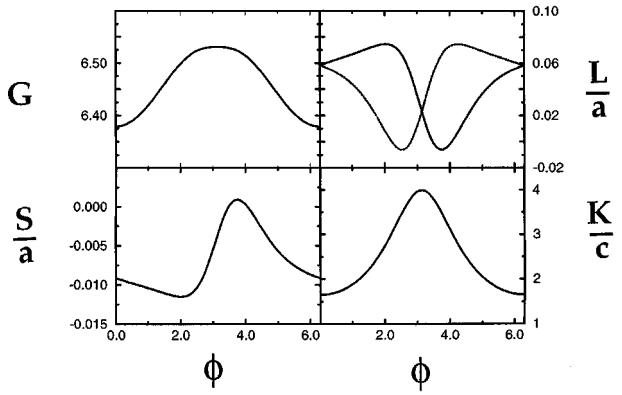

FIG. 13. Results for a clean interferometer, which lacks mirror symmetry along a horizontal line between the superconductors.

Eq. (9). In the absence of superconducting leads, or at a low enough temperature where open channels in any superconducting leads can be neglected, this further reduces to an equation of the form (1). For the simplest case of two normal reservoirs connected to a scattering region, the steady-state condition $I_1+I_2=0$ yields a further reduction to Eq. (2), with thermoelectric coefficients given by Eqs. (20)–(23).

The numerical results of Secs. IV and V are the first explicit realizations of the above formulas. Those of Sec. V are particularly interesting, since Andreev interferometers are now available in the laboratory. To date all theories and experiments on Andreev interferometers have focused exclusively on electrical properties. As shown in Fig. 10(a), the electrical conductance can have a negligible amplitude of oscillation, while in the same sample, the thermal conductance exhibits large-scale oscillations. This suggests that a complete understanding of quasiparticle interference effects requires a systematic study of a range of thermoelectric coefficients.

ACKNOWLEDGMENTS

This work was supported by the EC, the EPSRC, NATO, the Institute for Scientific Interchange, and the MOD. We thank Roberto Raimondi and Mark Leadbeater for detailed discussions.

[1] B. J. van Wees, A. Dimoulas, J. P. Heida, T. M. Klapwijk, W. v. d. Graaf, and G. Borghs, Physica B **203**, 285 (1994).
[2] P. G. N. de Vegvar, T. A. Fulton, W. H. Mallison, and R. E. Miller, Phys. Rev. Lett. **73**, 1416 (1994).
[3] H. Pothier, S. Gueron, D. Esteve, and M. H. Devoret, Physica B **203**, 226 (1994).
[4] V. T. Petrashov, V. N. Antonov, S. V. Maksimov, and R. Sh. Shaikhaidarov, Sov. Phys. JETP Lett. **59**, 551 (1994).
[5] Y. W. Kwong, K. Lin, P. J. Hakonen, M. S. Isaacson, and J. M. Parpia, Phys. Rev. B **44**, 462 (1991).
[6] P. Santhanam, C. C. Chi, S. J. Wind, M. J. Brady, and J. J. Buchignano, Phys. Rev. Lett. **66**, 2254 (1991).
[7] V. T. Petrashov, V. N. Antonov, and M. Persson, Phys. Scr. **T42**, 136 (1992).
[8] J.-J. Kim, J. Kim, S. Lee, H. J. Lee, K. W. Park, H. J. Shin, and E.-H. Lee, Physica B **194-196**, 1035 (1994).
[9] J.-J. Kim, J. Kim, S. Lee, H. J. Lee, K. W. Park, H. J. Shin, and E.-H. Lee (unpublished).
[10] A. Kastalasky, A. W. Kleinsasser, L. H. Greene, R. Bhat, and J. P. Harbison, Phys. Rev. Lett. **67**, 3026 (1991).
[11] B. J. van Wees, P. de Vries, P. Magnee, and T. M. Klapwijk, Phys. Rev. Lett. **69**, 510 (1992).
[12] V. T. Petrashov, V. N. Antonov, P. Delsing, and T. Claeson, Phys. Rev. Lett. **70**, 347 (1993).
[13] B. L. Al'tshuler and B. Z. Spivak, Sov. Phys. JETP **65**, 343 (1987).
[14] H. Nakano and H. Takayanagi, Solid State Commun. **80**, 997 (1991).
[15] S. Takagi, Solid State Commun. **81**, 579 (1992).
[16] C. J. Lambert, J. Phys.: Condens. Matter **5**, 707 (1993).
[17] V. C. Hui and C. J. Lambert, Europhys. Lett. **23**, 203 (1993).
[18] F. W. J. Hekking and Yu. V. Nazarov, Phys. Rev. Lett. **71**, 1625 (1993).
[19] Yu. V. Nazarov, Phys. Rev. Lett. **73**, 1420 (1994).
[20] A. V. Zaitsev, JETP Lett. **51**, 41 (1990).
[21] A. V. Zaitsev, Phys. Lett. A **194**, 315 (1994).
[22] N. R. Claughton and C. J. Lambert, Phys. Rev. B **51**, 11635 (1995).
[23] V. C. Hui and C. J. Lambert, J. Phys.: Condens. Matter **5**, L651 (1993).
[24] A. F. Volkov and T. M. Klapwijk, Phys. Lett. A **168**, 217 (1992).
[25] A. F. Volkov, A. V. Zaitsev, and T. M. Klapwijk, Physica C **210**, 217 (1993).
[26] I. K. Marmakos, C. W. J. Beenakker, and R. A. Jalabert, Phys. Rev. B **48**, 2811 (1993).
[27] A. Furusaki, H. Takayanagi, and M. Tsukada, Phys. Rev. Lett. **67**, 132 (1991).
[28] C. W. J. Beenakker and H. van Houten, Phys. Rev. Lett. **66**, 3056 (1991).
[29] P. F. Bagwell, Phys. Rev. B **46**, 12 573 (1992).
[30] A. Martin and C. J. Lambert, Phys. Rev. B **51**, 17 999 (1995); **51**, L221 (1994).
[31] J. Sanchez-Canizares and F. Sols, J. Phys.: Condens. Matter **7**, L317 (1995).
[32] U. Sivan and Y. Imry, Phys. Rev. B **33**, 551 (1986).
[33] P. Streda, J. Phys.: Condens. Matter **1**, 1025 (1989).
[34] P. N. Butcher, J. Phys.: Condens. Matter **2**, 4869 (1990).
[35] H. van Houten, L. W. Molenkamp, C. W. J. Beenakker, and C. T. Foxon, Semicond. Sci. Technol. **7**, B215 (1992).
[36] A. F. Andreev, Sov. Phys. JETP **19**, 1228 (1964).
[37] For a discussion of various formulas applicable to normal systems, see M. Büttiker, IBM J. Res. Dev. **32**, 317 (1988).
[38] C. J. Lambert, J. Phys.: Condens. Matter **3**, 6579 (1991).
[39] C. J. Lambert, V. C. Hui, and S. J. Robinson, J. Phys.: Condens. Matter **5**, 4187 (1993).